Neuron, Volume *109*

Supplemental information

Stress undermines reward-guided cognitive performance through synaptic depression in the lateral habenula

Alvaro Nuno-Perez, Massimo Trusel, Arnaud L. Lalive, Mauro Congiu, Denise Gastaldo, Anna Tchenio, Salvatore Lecca, Mariano Soiza-Reilly, Claudia Bagni, and Manuel Mameli

Nuno-Perez et al., Supplemental Figure 1

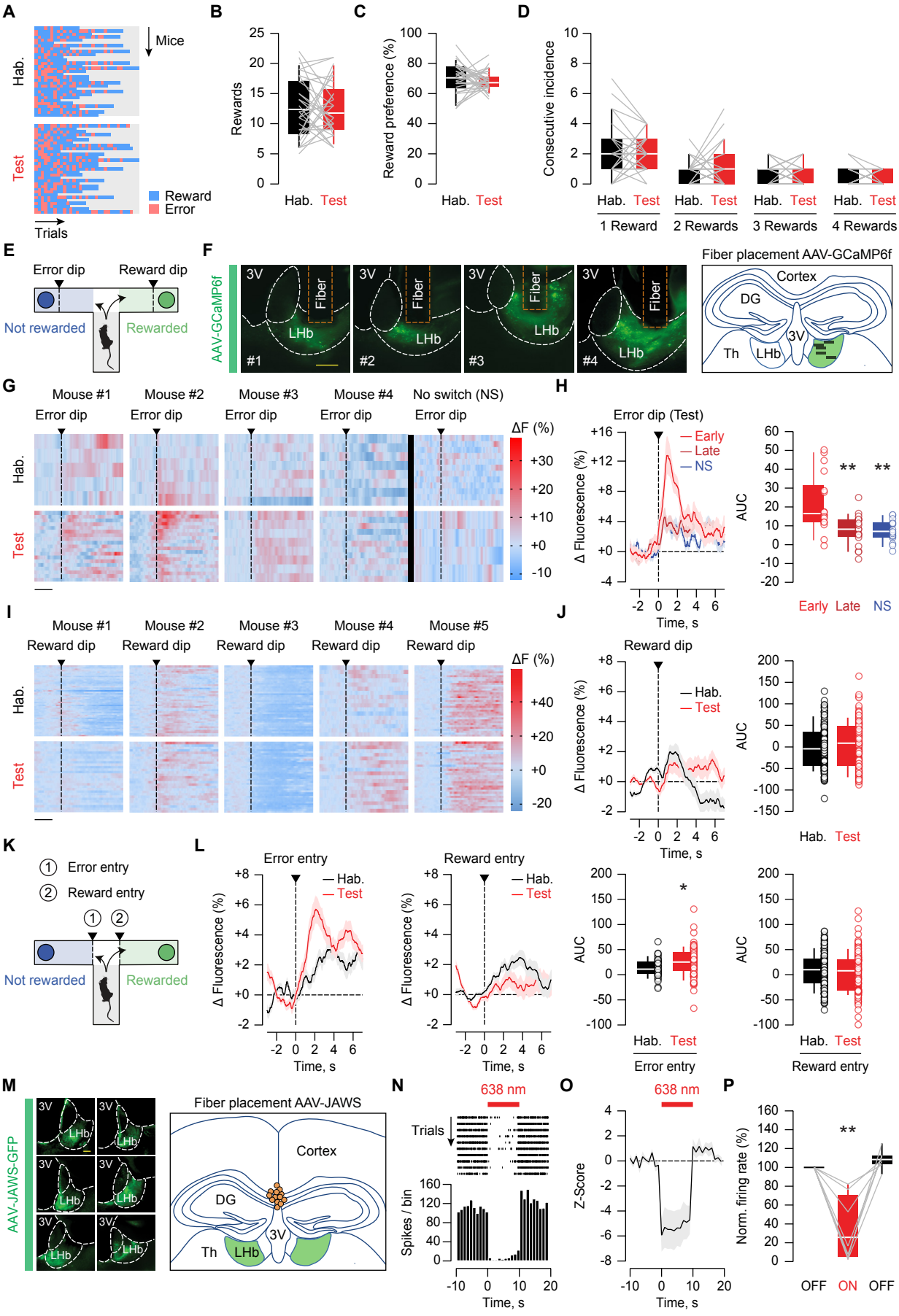

Figure S1. Behavioral, photometric and optogenetic analysis of LHb neurons during the T-maze task. Related to Figure 1.

(**A**) Single-mouse performance during habituation and test session (n=31 mice).

(**B**) Box and scatter plots of the reward incidence during habituation (black: n=31 mice, 12.74±0.8884) and test session (red: n=31 mice, 12.52±0.8137).

(**C**) Box and scatter plots of the reward preference during habituation (black: n=31 mice, 69.93±1.885) and test session (red: n=31 mice, 68.05±1.169).

(**D**) Box and scatter plots of the consecutive error incidence during habituation (black: n=31 mice, 2.0968±0.3172 for 1 error, 0.8387±0.1298 for 2 errors, 0.6774±0.1239 for 3 errors, and 0.3548±0.1075 for 4 errors) and test session (red: n=31 mice, 2.1613±0.2095 for 1 error, 1.2258±0.2268 for 2 errors, 0.5161±0.1279 for 3 errors, and 0.4194±0.0886 for 4 errors).

(**E**) Schematic of the behavioral task.

(**F**) Injection sites of AAV-GCaMP6f and fiber implantation above the site of injection (scale bar: 100 µm) in the cohort of mice employed for photometric experiments (Figure 1F). Coronal schematic depicting the approximate sites of fiber placement (black rectangles: n=5 mice).

(**G**) Single-mouse heat maps of LHb fluorescence aligned to the entry into the non-rewarded container (error dip) during habituation and test session (scale bar: 2 s).

(**H**) Time course of the average LHb fluorescence aligned to the entry into the non-rewarded container (error dip) during early and late trials of the test session, and during test trials in which the non-rewarded arm was not switched (NS). Box and scatter plots of the area under the curve (AUC) during early (light red: n=5 mice/17 trials, 21.8±3.769), late (dark red: n=5 mice/19 trials, 7.989±1.857) and no-switch trials during the test session (blue, NS: n=4 mice/15 trials, 7.274±1.517). One-way ANOVA ($F_{2,48}$=9.84) with Holm-Sidak correction (**p<0.01, comparisons against early).

(**I**) Single-mouse heat maps of LHb fluorescence aligned to the entry into the rewarded container (reward dip) during habituation and test session (scale bar: 2 s).

(**J**) Time course of the average LHb fluorescence aligned to the entry into the rewarded container (reward dip) during habituation and test session. Box and scatter plots of the area under the curve (AUC) during habituation (black: n=5 mice/186 trials, -0.3678±3.565) and test session (red: n=5 mice/149 trials, 5.404±4.376).

(**K**) Schematic of the behavioral task.

(**L**) Time course of the average LHb fluorescence during habituation and test session aligned to the entry into the non-rewarded and rewarded arms. Box and scatter plots of the area under the curve (AUC) during habituation (black: n=5 mice/46 trials, 13.6299±2.6152 for entry into non-rewarded arm; n=5 mice/186 trials, 10.1795±2.4401 for entry into rewarded arm) and test session (red: n=5 mice/74 trials, 25.0754±3.4268 for entry into non-rewarded arm; n=5 mice/150 trials, 4.3685±3.1677 for entry into rewarded arm). Mann-Whitney test (U=1228, *p<0.05).

(**M**) Representative injection sites of AAV-JAWS (scale bar: 100 µm) in the cohort of mice employed for behavioral experiments (Figure 1I). Coronal schematic depicting the approximate sites of fiber placement for the optical activation of JAWS (orange circles: n=13 mice).

(**N**) Raster plot and peri-stimulus time histogram of an example LHb neuron for the *in vivo* validation of JAWS photoactivation.

(**O**) Time course of the average z-score of spontaneous firing activity during red light treatment (n=2 mice/7 cells).

(**P**) Box and scatter plots of the normalized firing rate during (red: ON, 34.7±13.21) and after (black: OFF, 108.6±3.782) red light treatment (n=2 mice/7 cells). One-way repeated measures ANOVA ($F_{1.096,6.574}$=24.37) with Holm-Sidak correction (**p<0.01, ON versus OFF).

Data are represented with heat maps, box plots (median and quartiles) or mean±SEM.

Nuno-Perez et al., Supplemental Figure 2

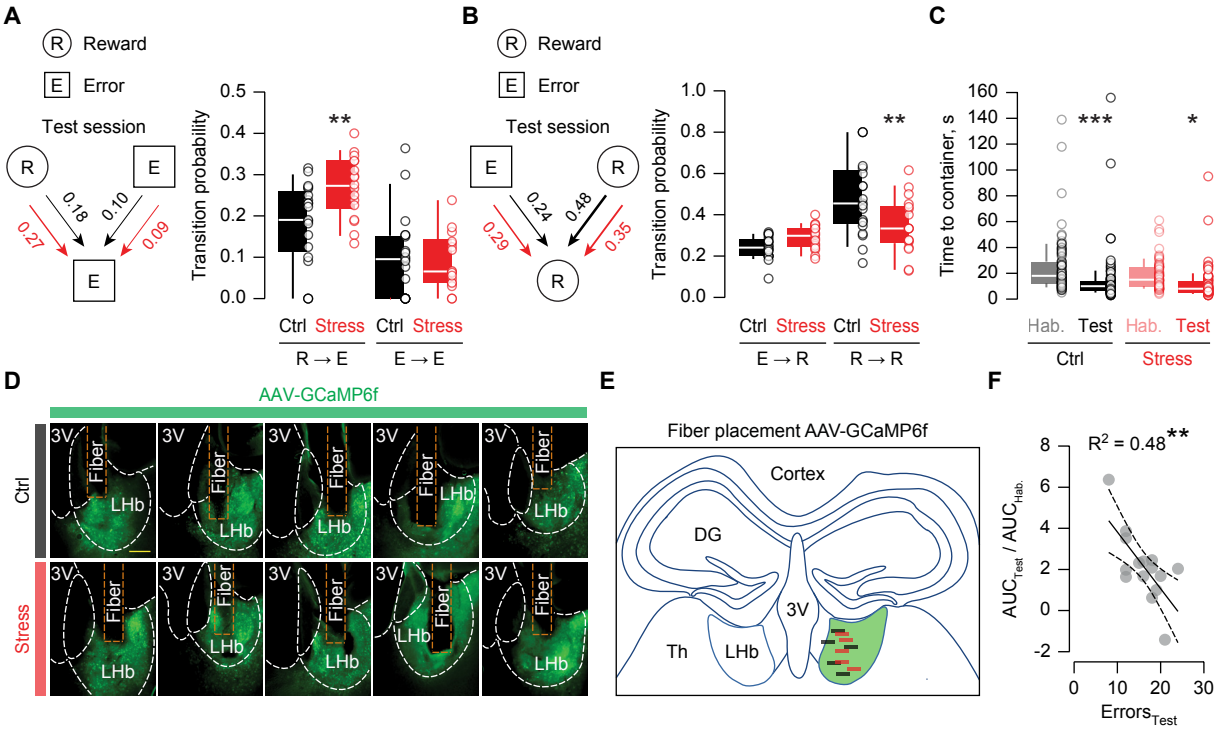

Figure S2. Behavioral and photometric analysis upon stress exposure. Related to Figure 2.

(**A**) Diagram displaying average transition probabilities to error choice during the test session. Box and scatter plots of transition probabilities to error choice in control (black: n=20 mice, 0.1817±0.02232 for R→E and 0.0973±0.02289 for E→E) and stressed mice (red: n=17 mice, 0.27±0.01914 for R→E and 0.08755±0.01605 for E→E). Two-way repeated measures ANOVA ($F_{1,35}$=3.214) with Sidak correction (**p<0.01, control versus stress).

(**B**) Diagram displaying average transition probabilities to reward choice during the test session. Box and scatter plots of transition probabilities to reward choice in control (black: n=20 mice, 0.241±0.01213 for E→R and 0.48±0.04154 for R→R) and stressed mice (red: n=17 mice, 0.2937±0.01448 for E→R and 0.3487±0.03276 for R→R). Two-way repeated measures ANOVA ($F_{1,35}$=3.214) with Sidak correction (**p<0.01, control versus stress).

(**C**) Box and scatter plots of the time to reach the arm containers in control (black: n=20 mice/100 trials, 23.87±2.015 during habituation; n=20 mice/100 trials, 13.56±1.877 during test) and stressed mice (red: n=15 mice/75 trials, 18.16±1.283 during habituation; n=17 mice/84 trials, 11.36±1.351 during test). Two-way ANOVA ($F_{1,355}$=23.7) with Sidak correction (***p<0.001, *p<0.05, habituation versus test).

(**D**) Injection sites of AAV-GCaMP6f and fiber implantation above the site of injection (scale bar: 100 µm) in the cohort of mice employed for photometric experiments (Figure 2C).

(**E**) Coronal schematic depicting the approximate sites of fiber placement (control: black rectangles, n=5 mice; stress: red rectangles, n=5 mice).

(**F**) Correlation plot between error incidence during the test session and LHb fluorescence aligned to the entry into the non-rewarded container (n=15 mice: 5 naïve mice from Figure 1F, 5 control mice from Figure 2C and 5 stressed mice from Figure 2C). Pearson correlation (R^2=0.4842, $F_{1,13}$=12.21, **p<0.01).

Data are represented with box plots (median and quartiles) or mean±SEM.

Nuno-Perez et al., Supplemental Figure 3

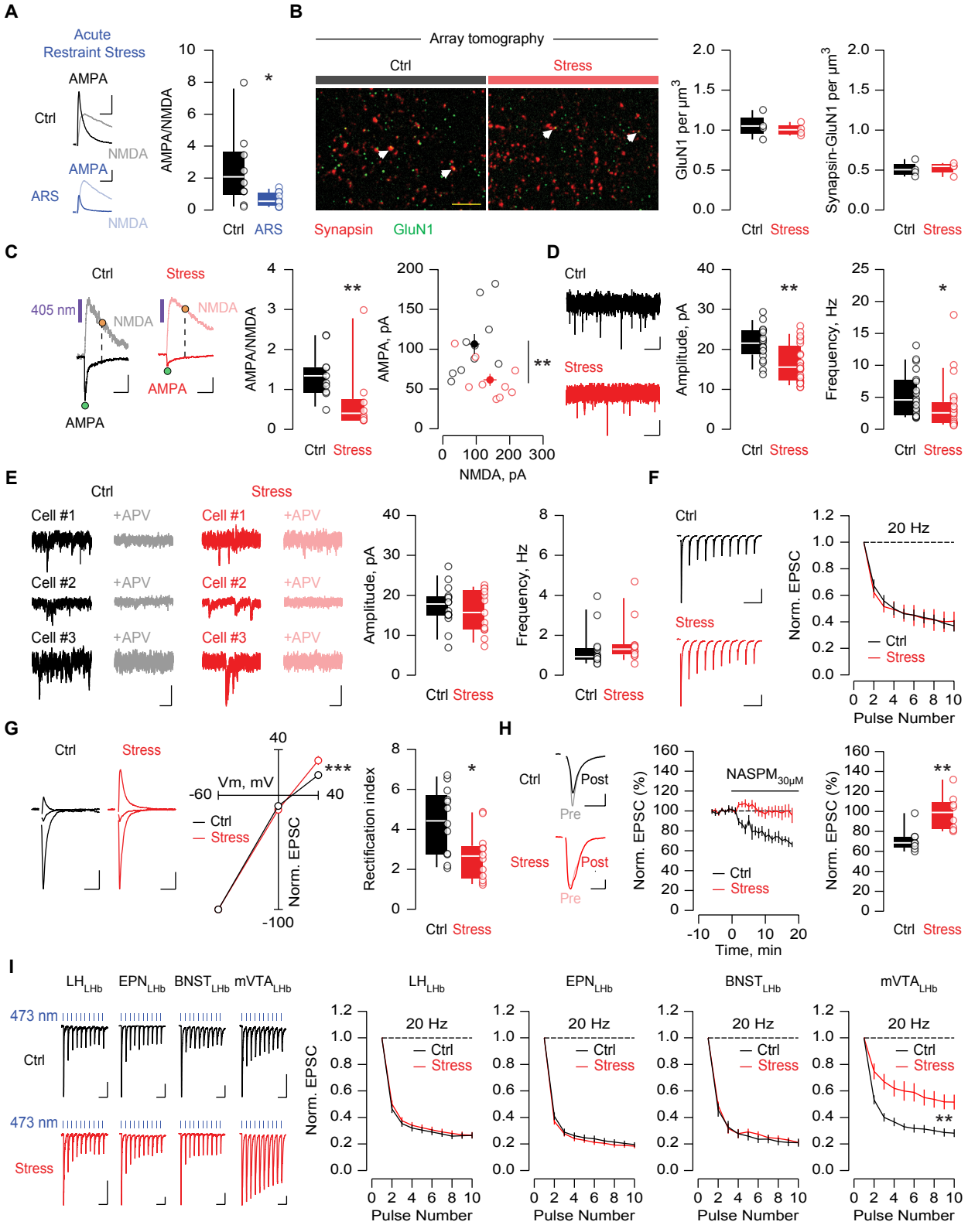

Figure S3. Stress reduces habenular AMPAR transmission. Related to Figure 2 and Figure 3.

(**A**) Example traces of AMPA/NMDA (+40 mV; scale bars: 50 pA, 10 ms). Box and scatter plots of AMPA/NMDA from control (black: n=2 mice/9 cells, 2.51±0.8158) and restrained mice (ARS, blue: n=3 mice/11 cells, 0.6564±0.1283). Mann-Whitney test (U=19, *p<0.05).

(**B**) Array tomography images obtained from single 100-nm slices immunolabeled against Synapsin (red) and GluN1 (green) (scale bar: 5 µm). White arrows indicate representative puncta showing co-localization of both markers. Box and scatter plots of the number of puncta per μm^3 in control (black: n=4 mice, 1.053±0.07596 for GluN1 and 0.5085±0.04607 for Synapsin/GluN1) and stressed mice (red: n=4 mice, 1.004±0.03689 for GluN1 and 0.5245±0.03795 for Synapsin/GluN1).

(**C**) Example traces of AMPA/NMDA with single-photon MNI-glutamate uncaging (-60/+40 mV; scale bars: 50 pA, 100 ms). Box and scatter plots of AMPA/NMDA from control (black: n=3 mice/10 cells, 1.372±0.1917) and stressed mice (red: n=2 mice/9 cells, 0.7061±0.2958). Scatter plot of absolute amplitudes in control (black: 106.4±13.28 for AMPAR and 94.29±15.79 for NMDAR) and stressed mice (red: 61.46±7.942 for AMPAR and 141.1±20.67 for NMDAR). Mann-Whitney test (U=13, **p<0.01).

(**D**) Example traces of AMPAR-mediated miniature EPSC recordings (mEPSC; -60 mV; scale bars: 10 pA, 250 ms). Box and scatter plots of mEPSC amplitude and frequency from control (black: n=3 mice/19 cells, 21.39±0.9497 for amplitude and 5.403±0.817 for frequency) and stressed mice (red: n=3 mice/23 cells, 16.5±1.003 for amplitude and 3.557±0.8387 for frequency). Mann-Whitney test (amplitude: U=98; frequency: U=127) (**p<0.01, *p<0.05).

(**E**) Example traces of NMDAR-mediated spontaneous EPSC recordings (sEPSC; -60 mV; scale bars: 20 pA, 100 ms), before and after bath application of the NMDAR antagonist APV. Box and scatter plots of sEPSC amplitude and frequency from control (black: n=2 mice/15 cells, 17.39±1.33 for amplitude and 1.279±0.2438 for frequency) and stressed mice (red: n=2 mice/13 cells, 15.8±1.495 for amplitude and 1.593±0.3034 for frequency).

(**F**) Example traces of AMPAR EPSC trains (-50 mV; scale bars: 50 pA, 100 ms). Plot of normalized EPSC amplitudes from control (black: n=2 mice/12 cells) and stressed mice (red: n=2 mice/12 cells).

(**G**) Example traces of AMPAR currents (-60/+0/+40 mV; scale bars: 50 pA, 10 ms). Current-voltage relationship, box and scatter plots of rectification index from control (black: n=2 mice/12 cells, 4.422±0.4847) and stressed mice (red: n=2 mice/12 cells, 2.663±0.359). Two-way repeated measures ANOVA ($F_{1,22}$=2.693) with Sidak correction (***p<0.001); Mann-Whitney test (U=28, *p<0.05).

(**H**) Example traces of AMPAR currents (-50 mV; scale bars: 50 pA, 5 ms). Time course, box and scatter plots of the NASPM sensitivity (30 µM) of AMPAR currents from control (black: n=3 mice/8 cells, 71.5±4.241) and stressed mice (red: n=3 mice/8 cells, 98.88±6.391). Mann-Whitney test (U=4, **p<0.01).

(**I**) Example traces of input-specific (Channelrhodopsin-2) AMPAR EPSC trains (-60 mV; scale bars: 50 pA, 100 ms). Plots of normalized EPSC amplitudes from control (black: LH, n=2 mice/24 cells; EPN, n=2 mice/29 cells; BNST, n=4 mice/34 cells; mVTA, n=2 mice/32 cells) and stressed mice (red: LH, n=3 mice/33 cells; EPN, n=2 mice/27 cells; BNST, n=2 mice/23 cells; mVTA, n=3 mice/43 cells). Two-way repeated measures ANOVA ($F_{1,73}$=10.59, **p<0.01, control versus stress interaction).

Data are represented with box plots (median and quartiles) or mean±SEM.

Nuno-Perez et al., Supplemental Figure 4

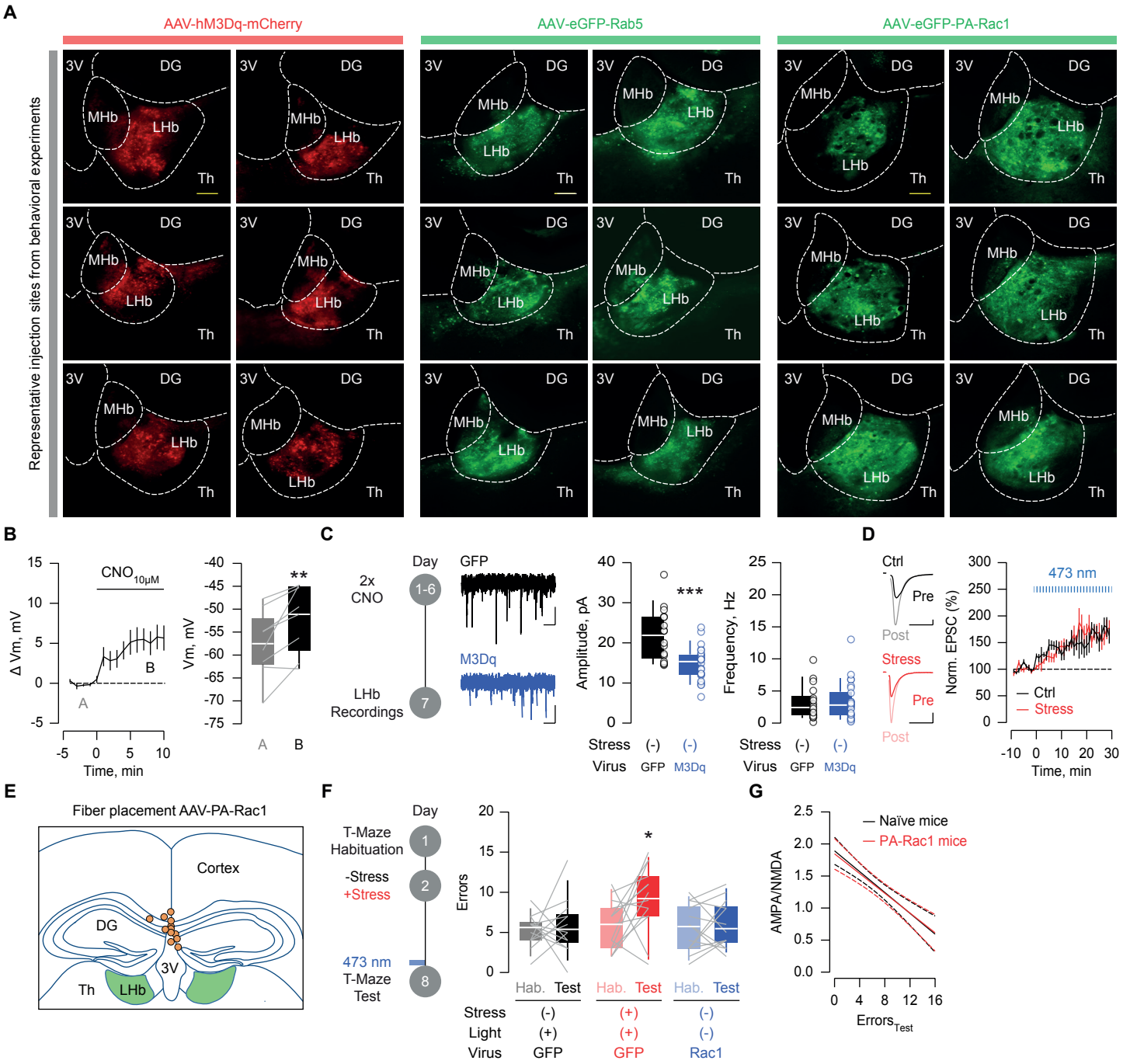

Figure S4. Validation of viral manipulations. Related to Figure 4.

(**A**) Representative injection sites of AAV-hM3Dq (scale bar: 100 μm), AAV-Rab5 (scale bar: 100 μm) and AAV-PA-Rac1 (scale bar: 50 μm) in the cohort of mice employed for behavioral experiments (Figure 4C, 4F and 4H).

(**B**) Time course of the change in membrane potential in LHb neurons upon bath application of CNO (10 μM). Box and scatter plots of the membrane potential before (grey: A, -57.53±2.643) and after (black: B, -52.06±2.654) CNO treatment (n=3 mice/8 cells). Paired student's t-test (t_7=3.536, **p<0.01).

(**C**) Experimental timeline. Example traces of AMPAR-mediated miniature EPSC recordings (mEPSC; -60 mV; scale bars: 10 pA, 250 ms). Box and scatter plots of mEPSC amplitude and frequency from GFP (black: n=2 mice/16 cells, 21.84±1.615 for amplitude and 3.097±0.6359 for frequency) and M3Dq mice (blue: n=3 mice/25 cells, 14.81±0.8312 for amplitude and 3.344±0.5879 for frequency). Mann-Whitney test (U=76, ***p<0.001).

(**D**) Example traces of AMPAR currents during the *ex vivo* validation of PA-Rac1 photoactivation (-60 mV; scale bars: 50 pA, 10 ms). Time course of the amplitude of AMPAR currents from control (black: n=2 mice/9 cells) and stressed mice (red: n=2 mice/7 cells), before and after blue light delivery (1 Hz, 150 ms). Two-way repeated measures ANOVA ($F_{38,532}$=6.577, ***p<0.001, time interaction).

(**E**) Coronal schematic depicting the approximate sites of fiber placement for the optical activation of PA-Rac1 (orange circles: n=12 mice).

(**F**) Experimental timeline. Box and scatter plots of the error incidence in GFP mice subjected to control/light (black: n=13 mice, 5.2308±0.5456 during habituation and 5.7692±0.9176 during test), GFP mice subjected to stress/light (red: n=14 mice, 5.9286±0.7657 during habituation and 9.2143±1.0747 during test) and PA-Rac1 mice subjected to control/no-light (blue: n=13 mice, 5.4615±0.7966 during habituation and 5.9231±0.7879 during test). Two-way repeated measures ANOVA ($F_{1,37}$=3.952) with Sidak correction (*p<0.05, habituation versus test).

(**G**) Overlay of the correlation analysis between error incidence and AMPA/NMDA from naïve (black, Figure 1J: R^2=0.833, $F_{1,9}$=44.89, ***p<0.001) and stressed PA-Rac1 mice (red, Figure 4I: R^2=0.9388, $F_{1,4}$=61.38, **p<0.01). Pearson correlation with test for slope comparison ($F_{1,13}$=0.06798, p=0.7984).

Data are represented with box plots (median and quartiles) or mean±SEM.